Research Square

Preprints are preliminary reports that have not undergone peer review.
They should not be considered conclusive, used to inform clinical practice,
or referenced by the media as validated information.

Flow cytometry-assisted optimization of culture conditions for the PCP-containing dinoflagellate Heterocapsa pygmaea: effects on cell growth and pigment fluorescence

Jiang-Ting Lu Chen
National Taiwan Ocean University
Chi-Cheng Huang
National Taiwan Ocean University
Hung-Yun Lin
National Taiwan Ocean University
VARUNRAJ RAJENDRAN
National Taiwan Ocean University
Jin-De Li
China Medical University
Yi-Jung Chen
National Taiwan Ocean University
Fat-Tin Agassi Sze
create goods biomedical co.,
Yen-Ling Chen
Fisheries Resarch Insistute, Ministry oF agriculture
Fan-Hua Nan
National Taiwan Ocean University
Mary Joy Libatique - Asprec
libatiquemaryjoy@yahoo.com

Isabela State University
Meng-Chou Lee
mengchoulee@email.ntou.edu.tw

National Taiwan Ocean University

Research Article

Keywords: bioprocess optimization, culture optimization, dinoflagellate, flow cytometry, Heterocapsa pygmaea, peridinin–chlorophyll a protein

Posted Date: November 10th, 2026

DOI: https://doi.org/10.21203/rs.3.rs-11660646/v1

License: This work is licensed under a Creative Commons Attribution 4.0 International License.
Read Full License

Additional Declarations: The authors declare no competing interests.

applied sciences

MDPI

Article

Flow cytometry-assisted optimization of culture conditions for the PCP-containing dinoflagellate Heterocapsa pygmaea: effects on cell growth and pigment fluorescence

Jiang-Ting Lu Chen[1], Chi-Cheng Huang[1], , Hung-Yun Lin[2,3], Varunraj Rajendran[1], Jin-De Li[4], Yi-Jung Chen[1,5], Fat-Tin Agassi Sze[1,6], Yen-Ling Chen[1,7], Fan-Hua Nan[1], Mary Joy Libatique-Asprec[8],* and Meng-Chou Lee[1,5],*

[1] Department of Aquaculture, National Taiwan Ocean University, Keelung City 20224, Taiwan; charles@algaeconversion.com (F.-T.A.S.); jeff80227@gmail.com (Y.-J.C.); bioreactor01@gmail.com (C.-C.H.); popogaga4125252@gmail.com (J.-T.L.C.); fhnan@mail.ntou.edu.tw (F.-H.N.) 21533008@mail.ntou.edu.tw (V.R.); mengchoulee@email.ntou.edu.tw (M.-C.L.)

[2] Bachelor Degree Program in Marine Biotechnology, National Taiwan Ocean University, Keelung 202301, Taiwan; hungyun@mail.ntou.edu.tw (H.-Y.L.)

[3] Taiwan Oceans Genome Center, National Taiwan Ocean University, Keelung 202301, Taiwan; hungyun@mail.ntou.edu.tw (H.-Y.L.)

[4] School of Medicine, College of Medicine, China Medical University, Taichung 406040, Taiwan; chindelee1@gmail.com (J.-D.L.)

[5] Center of Excellence for the Ocean, National Taiwan Ocean University, Keelung City 20224, Taiwan; mengchoulee@email.ntou.edu.tw (M.-C.L.)

[6] Create goods biomedical Co., Limited, Tainan City 700003, Taiwan; charles@algaeconversion.com (F.-T.A.S.)

[7] Aquaculture Division, Fisheries Research Institute, Ministry of Agriculture, Keelung 20246, Taiwan; 21433002@mail.ntou.edu.tw (Y.-L.C.)

[8] Institute of Fisheries—Freshwater Fisheries Center, Isabela State University, Echague, Isabela, Philippines; libatiquemaryjoy@yahoo.com (M.-J.L.A.)

* Correspondence: mengchoulee@email.ntou.edu.tw (M.-C.L.); mengchoulee@gmail.com (M.-C.L.); Tel.: +886-2-246222192 (ext. 5239); libatiquemaryjoy@yahoo.com (M.-J.L.A.).

Abstract

Dinoflagellates are promising sources of high-value light-harvesting proteins, but their commercial utilization remains limited by insufficiently optimized cultivation conditions and the lack of efficient physiological monitoring tools. This study aimed to enhance cell growth and peridinin–chlorophyll a–protein (PCP) performance in *Heterocapsa pygmaea* through a combined cultivation and monitoring framework. PCP was characterized using SDS-PAGE and HPLC, and environmental (temperature and light intensity) and nutritional (phosphorus, nitrogen, and iron) factors were systematically evaluated, with flow cytometry applied to simultaneously assess cell density and intracellular fluorescence intensity as a rapid in vivo indicator of PCP-associated physiological performance. The PCP preparation exhibited a molecular weight of 10–15 kDa and a pigment composition dominated by peridinin and chlorophyll a. The best-performing cultivation conditions within the tested ranges were 24 °C, 100 μmol photons m^{-2} s^{-1}, 60 μM phosphorus supplied as mixed sources, nitrate or mixed nitrogen conditions, and 17.55 μM iron. Incorporation of these parameters into a modified C5 medium significantly improved cell growth and fluorescence responses compared with conventional f/2 and K

media ($p < 0.05$). Combining cultivation optimization with flow cytometry-guided physiological monitoring is an effective strategy for improving PCP-associated fluorescence responses and establishes a scalable framework for dinoflagellate bioprocess development and industrial biotechnology applications.

Keywords: bioprocess optimization; culture optimization; dinoflagellate; flow cytometry; *Heterocapsa pygmaea*; peridinin–chlorophyll a protein

1. Introduction

Dinoflagellates are ecologically important microalgae that contribute substantially to marine primary productivity and biogeochemical cycling. Beyond their ecological roles, they have emerged as a promising source of high-value biomolecules, particularly light-harvesting pigment–protein complexes with distinctive optical and functional properties. Among these, the peridinin–chlorophyll a–protein (PCP) complex is of particular interest because of its high fluorescence quantum yield, broad excitation spectrum, and near-unity energy transfer efficiency, which make it highly suitable for applications in fluorescence-based diagnostics, biosensing, and photonic systems [22,23].

Despite its significant biotechnological potential, the practical use of PCP remains constrained by the lack of efficient and scalable production systems. Previous studies have primarily focused on the structural and photophysical characterization of PCP, particularly in model dinoflagellates such as Amphidinium carterae, whereas comparatively little attention has been paid to species such as *Heterocapsa pygmaea*, which possess distinct PCP forms and pigment compositions [15,16]. More importantly, few studies have integrated cultivation optimization with functional performance assessment, creating a gap between laboratory characterization and scalable process development.

Microalgal growth and pigment synthesis are strongly regulated by environmental conditions, such as temperature and light intensity, as well as nutrient availability, particularly nitrogen, phosphorus, and iron. These factors influence photosynthetic efficiency, metabolic activity, and pigment accumulation through interconnected physiological pathways [13,14]. However, dinoflagellates exhibit species-specific physiological plasticity, including flexible nutrient acquisition strategies and dynamic pigment regulation, which complicates the identification of optimal cultivation conditions. Consequently, many existing studies rely on single factor optimization or endpoint analyses that do not fully capture interactions among variables during cultivation.

In addition to cultivation constraints, conventional PCP quantification methods further limit process development. Extraction-based techniques can provide absolute pigment or protein concentrations, but they are labor-intensive, time-consuming, and poorly suited to repeated monitoring across multiple experimental conditions. These limitations reduce analytical throughput and slow down optimization workflows. Recent advances in microalgal biotechnology have therefore emphasized the value of high-throughput physiological screening tools that can more efficiently link culture conditions with intracellular responses.

Flow cytometry (FCM) has emerged as a powerful analytical platform for single-cell analysis of microalgal systems, enabling the simultaneous quantification of cell density and intracellular fluorescence signatures [10, 17]. In PCP-producing dinoflagellates, these fluorescence signatures provide an informative indicator of intracellular pigment status and photosynthetic function without requiring destructive extraction procedures. This capability enables flow cytometry-guided monitoring of PCP-associated fluorescence and allows rapid comparison of culture performance across multiple environmental and nutritional conditions. Compared with conventional quantification approaches, FCM offers a scalable strategy for dynamic physiological screening and accelerated process optimization.

From a bioprocess engineering perspective, integrating analytical monitoring with cultivation optimization is increasingly recognized as an effective strategy for accelerating the development of scalable microalgal production systems. Recent advances in microalgal biotechnology have emphasized the use of physiological indicators, sensor-based monitoring, and high-throughput analytical platforms to rapidly evaluate culture performance under multiple environmental and nutritional conditions [12, 18]. Such approaches improve process efficiency by enabling data-driven optimization and reducing the time required for experimental screening. Despite these advances, comparable integrated cultivation-monitoring frameworks remain limited in dinoflagellate systems, particularly among PCP-producing species.

H. pygmaea is a promising yet underutilized dinoflagellate species because of its ability to produce PCP with favorable fluorescence properties. Its cultivation requirements and PCP production dynamics remain poorly understood, and no study has yet established a framework that simultaneously optimizes the species' cell growth and PCP-associated functional performance.

Therefore, the present study aimed to (i) characterize the molecular and pigment composition of PCP *from H. pygmaea* and (ii) establish an integrated cultivation optimization framework through the systematic evaluation of environmental (temperature and light) and nutritional (nitrogen, phosphorus, and iron) factors affecting cell growth and PCP-associated fluorescence performance. A central feature of this work is the use of flow cytometry-guided monitoring as an in vivo analytical platform for the simultaneous assessment of cell density and PCP-associated fluorescence responses. By combining cultivation optimization with physiological signal tracking, this study establishes an integrated dinoflagellate bioprocess optimization framework for enhanced PCP-associated performance. These findings provide biological and bioprocess insights into *H. pygmaea* cultivation while demonstrating the value of flow cytometry-guided physiological monitoring for accelerating the development of a PCP-oriented microalgal process.

2. Materials and Methods

2.1. Microalgal Strain and Culture Conditions

The experimental strain Heterocapsa pygmaea (K-0961) was purchased from the Norwegian Culture Collection of Algae (NORCCA; Norwegian Institute for Water Research & University of Oslo, Oslo, Norway). Stock cultures were maintained in a Tominaga (Taipei, Taiwan) temperature-controlled plant growth chamber at 24 °C under white LED T8 lighting at a light intensity of 100 μmol photons m^{-2} s^{-1} with a 12 h:12 h light:dark photoperiod. Cultures were grown in K medium [1] prepared with autoclaved (121 °C, 20 min) seawater, with salinity adjusted to 30 ppt.

Between experiments, the stock was subcultured approximately every four weeks by inoculating exponential-phase culture into fresh K medium to keep the strain in a stable growth state. Culture flasks were shaken by hand daily to resuspend the cells, and no active aeration was applied. At the start of each experiment, the initial inoculation density was approximately 1.00×10^5 cells mL^{-1}, and the culture period was 8 days. The temperature and light-intensity experiments were carried out in a culture volume of 200 mL, whereas the phosphorus, nitrogen, and iron concentration experiments and the medium comparison experiment used 400 mL.

2.2. PCP Characterization

2.2.1. Protein Molecular Weight Determination

The molecular weight of peridinin–chlorophyll a–protein (PCP) was determined by SDS-PAGE according to Laemmli [2]. Protein samples (1 μg) were mixed with 5× loading buffer and denatured at 95 °C for 10 min. Electrophoresis was performed using a 15% polyacrylamide gel at 80 V for stacking, followed by 100 V for separation. Protein bands were visualized by Coomassie Brilliant Blue staining and compared with a prestained molecular weight marker.

2.2.2. Pigment Composition Analysis

The pigment composition of PCP was analyzed using high-performance liquid chromatography (HPLC), with the analytical conditions following those reported by Chen et al. [3]. Algal biomass was harvested by centrifugation and extracted using acetone: methanol (7:2, v/v) with bead-assisted cell disruption. Extracts were filtered through 0.2 μm PTFE syringe filters prior to analysis. HPLC separation was performed using a reverse-phase C18 column with gradient elution under controlled flow conditions. Pigments were detected at 475 nm and 665 nm to identify peridinin and chlorophyll a, respectively.

2.3. Experimental Design for Integrated Culture Optimization

A sequential optimization framework was employed to systematically evaluate the individual and combined effects of environmental and nutritional variables on culture productivity and PCP-associated fluorescence responses in H. pygmaea. Optimization experiments were designed to identify cultivation conditions that maximized both cell growth and fluorescence-based cellular responses while maintaining physiological stability. All experiments were conducted in sterilized seawater (30 ppt) using K medium as the basal medium, unless otherwise specified. The complete compositions of the K, f/2, and modified C5 media are provided in the Supplementary Materials.

Cultures were grown in Erlenmeyer flasks (200–400 mL working volume) under a 12:12 h light: dark photoperiod with continuous aeration. Each treatment was conducted in quadruplicate (n = 4), with an initial inoculation density of approximately 1.0 photoperiod. Each treatment was conducted in quadruplicate (n = 4), with an initial inoculation density of approximately 1.00×10^5 cells mL^{-1}. The experiments were carried out over 8 days, with sampling performed on days 0, 2, 4, 6, and 8.

2.3.1. Temperature Optimization

Cultures were incubated at 16, 20, 24, and 28 °C under 60 μmol photons m^{-2} s^{-1} to evaluate the effects of temperature on growth. Cell density and specific growth rate (SGR) were measured on days 0 and 8. Response surface methodology (RSM) [4] was used to determine the optimal temperature conditions.

2.3.2. Light Intensity Optimization

Following temperature optimization, cultures were exposed to light intensities of 20, 60, 100, and 140 μmol photons m^{-2} s^{-1} at 24 °C. Growth and fluorescence responses were monitored, and optimal irradiance conditions were identified using RSM.

2.3.3. Phosphorus Optimization

(a) Concentration

Phosphorus concentrations of 10, 30, 60, and 120 μM were tested under optimal temperature and light conditions. Samples were collected every two days to measure cell density, relative fluorescence intensity, and pH. Total phosphorus in the medium was also analyzed to assess nutrient utilization.

(b) Source

Phosphorus sources included inorganic ($NaH_2PO_4 \cdot 2H_2O$), organic (Na_2β-glycerophosphate), and mixed (1:1) forms. All treatments were standardized to equivalent phosphorus levels.

2.3.4. Nitrogen Optimization

(a) Comparison of nitrogen sources.

Nitrogen sources (nitrate, ammonium, and urea) were evaluated at equivalent nitrogen concentrations.

(*b) Nitrogen substitution strategy.*

A mixed nitrogen treatment (50% nitrate + 50% urea) was tested to assess whether a cost-effective substitution could be achieved without compromising performance.

2.3.5. Iron Optimization

Iron concentrations of 0, 1.46, 2.93, 5.85, 11.7, and 17.55 μM were tested. Growth performance, fluorescence, and pH were monitored every 2 days. RSM analysis was applied to identify the best-performing iron level within the range tested.

2.3.6. Integrated Medium Formulation and Validation

Based on the optimal conditions, a modified culture medium (C5) was developed. Its performance was compared with that of conventional f/2 [5] and K media under identical conditions. Growth, SGR, and PCP-associated fluorescence were monitored by flow cytometry.

2.4. Flow Cytometry-Based Analysis

Cell density and pigment fluorescence were measured with an Attune NxT acoustic focusing flow cytometer (Thermo Fisher Scientific) [6]. Samples were excited with a 488 nm blue laser (50 mW), and fluorescence was collected through a 695/40 nm filter (BL3 channel, corresponding to PerCP). For each sample, 1 mL was taken and mixed thoroughly before loading to prevent cells from accumulating at the liquid surface. The acquisition volume was 200 μL, the flow rate was 200 μL min^{-1}, and the stop volume was set to 100 μL; recording began once the flow rate had stabilized.

Detector voltages were set to FSC 250, SSC 300, and BL3 240, and the acquisition threshold was set to 400. A minimum of 10,000 events was acquired per sample. Gating was performed in three stages. First, the high-fluorescence population (R1) was gated on the fluorescence histogram to distinguish algal cells from debris. Second, the R1 population was displayed on an FSC versus SSC dot plot, and a population with similar cell size and complexity (R2) was gated. Finally, a further gate (R3) was drawn on a histogram within R2. The accuracy of the gated populations was verified using the imaging function of an imaging flow cytometer (Attune CytPix), confirming that the gated events were indeed H. pygmaea cells. Cell density was calculated as cells mL^{-1} from the number of events in the R1 gate, using the formula: cell density (cells mL^{-1}) = R1 count × 10 × dilution factor, where the constant 10 converts counts from the 100 μL stop volume to per millilitre (1000 μL ÷ 100 μL); if a sample was diluted, the result was additionally multiplied by its dilution factor. Relative fluorescence intensity was expressed as RIChl (relative index of chlorophyll, %), calculated as follows: a population with similar cell size and complexity (R2) was first gated on the FSC versus SSC plot, a sub-population with stronger fluorescence (R3) was then gated on the fluorescence histogram within R2, and RIChl was obtained as: RIChl (%) = (number of particles in the R3 gate ÷ number of particles in the R2 gate) × 100. This index represents the proportion of cells within the gated population whose fluorescence falls within the high-fluorescence range, and was used to compare the relative expression of PCP-related fluorescence among culture conditions. All instrument settings were kept constant for every sample throughout the study to ensure comparability among treatments. Representative fluorescence histograms generated during optimization experiments are provided in the Supplementary Materials (Figures S1–S7).

The following parameters were calculated:

- Cell density (cells mL^{-1})
- Relative fluorescence intensity (PCP-associated(RIChl, %; PCP-associated fluorescence proxy)
- Specific growth rate (SGR; % day^{-1})

SGR was calculated as follows:

$$SGR = [(\ln N_2 - \ln N_1) / (t_2 - t_1)] \times 100 \quad \textbf{(1)}$$

where N_1 and N_2 represent the initial and final cell densities (cells mL^{-1}), respectively, and $(t_2 - t_1)$ represents the cultivation period in days [7]. Growth was therefore assessed on the basis of cell density and specific growth rate; biomass productivity (e.g., dry weight or bio volume per unit volume per time) was not measured in this study [6,7].

2.5. Rationale for Flow Cytometry-Based Assessment

Flow cytometry (FCM) was employed as a primary analytical tool because it enables rapid, high-throughput analysis of microalgal cultures at single-cell resolution. Conventional extraction-based quantification of pigment–protein complexes, although capable of providing absolute concentrations (e.g., mg L^{-1}), is labor-intensive and limits analytical throughput [10].

Recent studies have demonstrated that fluorescence-based measurements obtained through FCM provide valuable indicators of intracellular pigment status, physiological condition, and stress-associated cellular responses in microalgae, supporting their use in rapid cultivation assessment and process optimization [10,11,12].

In this study, fluorescence signals associated with PCP were used as relative indicators of functional performance across culture conditions. This approach enables efficient screening of environmental and nutritional parameters and rapid process optimization. While absolute PCP quantification remains important for downstream validation, FCM provides a scalable and effective strategy for early stage optimization.

2.6. Supporting Analyses

2.6.1. Total Phosphorus Analysis

Total phosphorus was determined by the molybdenum blue method [8] following persulfate digestion [9], with absorbance measured at 880 nm.

2.6.2. pH Measurement

Culture pH was monitored throughout cultivation using a calibrated digital pH meter to assess changes associated with nutrient assimilation and photosynthetic carbon fixation.

2.7. Statistical and Optimization Analysis

2.7.1. Statistical Analysis

All results are presented as mean ± standard deviation (SD) of four independent replicate cultures (n = 4) per treatment. Before analysis, normality of the data was assessed using the Shapiro–Wilk test and homogeneity of variance using Levene's test. Because each replicate culture was sampled repeatedly during cultivation (days 0, 2, 4, 6, and 8), measurements taken from the same culture at different time points are not independent of one another. Treatment comparisons were therefore made separately at each sampling day using one-way analysis of variance (ANOVA), with the experimental treatment (temperature, light intensity, phosphorus concentration or source, nitrogen source, iron concentration, or culture medium) as the fixed factor. When the ANOVA indicated a significant treatment effect, differences between individual treatment means were identified using Tukey's honestly significant difference (HSD) post hoc test.

Changes over time within a treatment were described but were not tested statistically. Specific growth rate (SGR), which was calculated once for each culture over the cultivation period (Equation 1), was analyzed in the same way. Differences were considered statistically significant at $p < 0.05$ and are indicated by different letters in the figures. All statistical analyses were performed using SPSS Statistics 22 (IBM, Armonk, NY, USA).

2.7.2. Response Surface Methodology

Response surface methodology (RSM) [4] was used to describe how culture responses changed across the tested levels of temperature (Section 2.3.1), light intensity (Section 2.3.2), and iron concentration (Section 2.3.5), and to identify the optimum level of each factor within the range tested. In line with the sequential optimization framework described in Section 2.3, each factor was evaluated separately using the treatment levels listed in the corresponding section. Models were constructed using Design-Expert software (v12.0.0, Stat-Ease Inc., Minneapolis, MN, USA). For each factor, the measured response (Y; cell density or PCP-associated fluorescence) was fitted to a second-order polynomial model:

$$Y = \beta_0 + \sum\beta_i X_i + \sum\beta_{ii} X_i^2 + \sum\sum\beta_{ij} X_i X_j \quad \textbf{(2)}$$

where Y is the predicted response; β_0 is the intercept; β_i, β_{ii}, and β_{ij} are the linear, quadratic, and interaction coefficients, respectively; and X_i and X_j are the coded levels of the independent variables. The significance of each model and of its individual terms was tested by ANOVA (F-test, $p < 0.05$). Model adequacy was evaluated using the coefficient of determination (R^2), adjusted R^2, predicted R^2, and the lack-of-fit test, with a non-significant lack of fit ($p > 0.05$) taken to indicate that the model adequately described the experimental data. The fitted models were visualized as two-dimensional contour plots and three-dimensional response surface plots, and the optimum level of each factor was defined as the level giving the maximum predicted response. The model equations, ANOVA tables, and goodness-of-fit statistics for each response are provided in the Supplementary Materials.

3. Results

3.1. Characterization of Peridinin–Chlorophyll a–Protein (PCP)

The protein extracted from *H. pygmaea* was characterized to support its identification as peridinin–chlorophyll a–protein (PCP). SDS-PAGE analysis revealed a distinct protein band at approximately 10–15 kDa (Figure 1A). HPLC analysis further characterized the pigment composition of the complex, where a major peridinin peak was detected at 475 nm (~10.5 min retention time), and chlorophyll a was identified at 665 nm (~48.0 min) (Figure 1B).

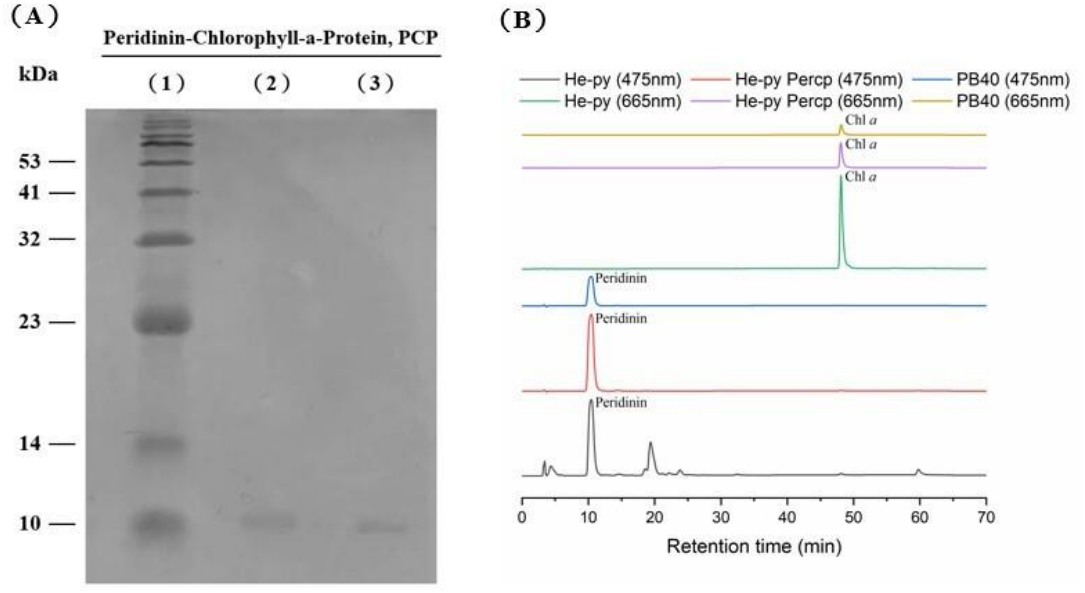


Figure 1. Characterization of peridinin–chlorophyll a–protein (PCP) in *Heterocapsa pygmaea*. (A) SDS-PAGE profile showing a distinct protein band at approximately 10–15 kDa, consistent with PCP. (B) RP-HPLC chromatograms detected at 475 nm and 665 nm supported the characteristic pigment composition of PCP, including peridinin and chlorophyll a.

3.2. Flow Cytometry-Based Assessment of Biomass and PCP-Associated Performance

Flow cytometry (FCM) enabled the simultaneous quantification of cell density and relative fluorescence intensity in *H. pygmaea*. Distinct algal populations were clearly resolved by FSC–SSC discrimination, allowing reliable separation of algal cells from debris. Fluorescence histograms obtained from the BL3-A (PerCP-associated) channel showed stable intracellular pigment-associated signals, while sequential gating and microscopic validation supported the accurate identification of *H. pygmaea* cells and the exclusion of background particles (Figure 2). Across treatments, fluorescence profiles closely paralleled cell density. Importantly, FCM also captured transient responses, showing a temporary fluorescence suppression under excess phosphorus and elevated iron conditions. Representative flow cytometry fluorescence histograms illustrate treatment-dependent shifts in intracellular fluorescence signals under different temperatures and light condition.

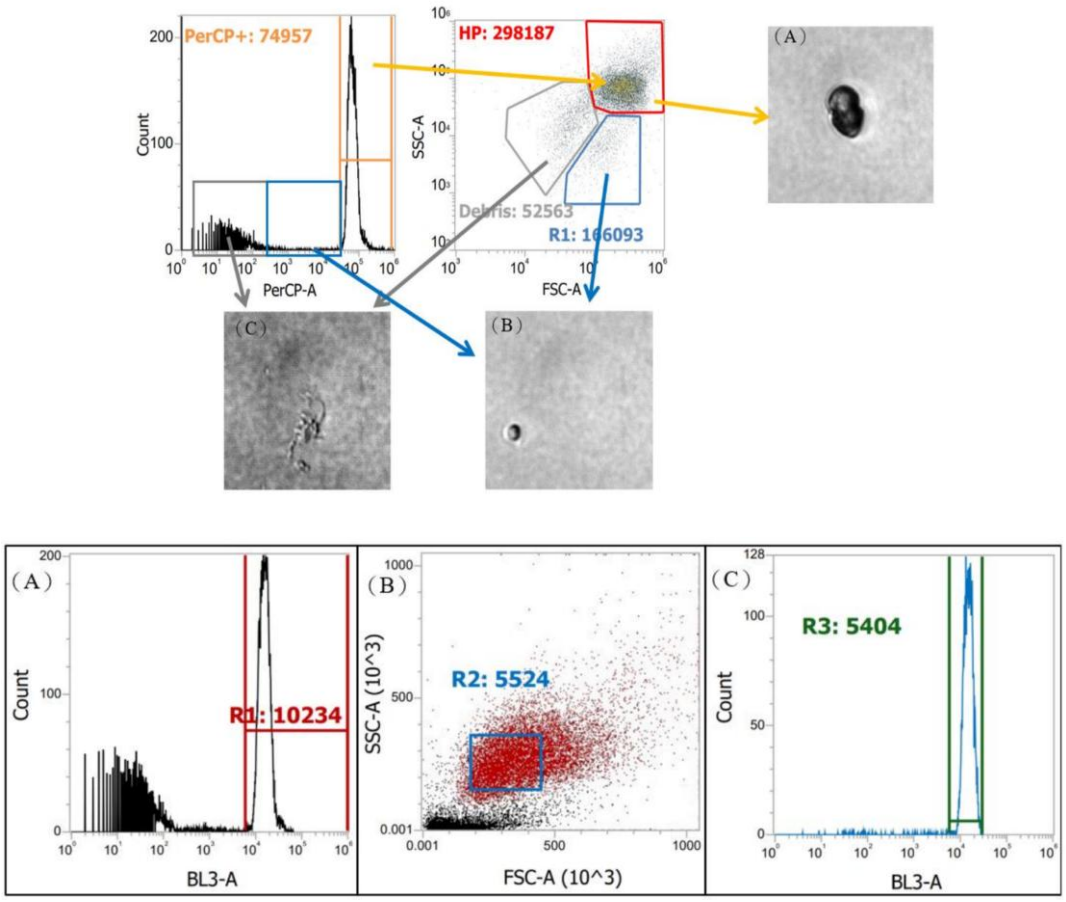


Figure 2. Flow cytometry-based analytical framework for assessing biomass and PCP-associated fluorescence in *Heterocapsa pygmaea*. The upper panels illustrate the sequential identification of *H. pygmaea* cells using PerCP-associated fluorescence, FSC–SSC discrimination, and microscopic validation of gated populations and excluded particles. The lower

panels show the gating workflow used for downstream analysis, including (A) fluorescence gating in the BL3-A channel, (B) FSC–SSC discrimination of algal cells, and (C) final fluorescence gating of selected populations.

3.3. Effects of Temperature and Light Intensity on Cell Growth

Temperature significantly affected the growth of *H. pygmaea*. After 8 days, both cell density and specific growth rate (SGR) were highest at 24 °C (Figure 3A–B), and response surface analysis confirmed approximately 24 °C as the thermal optimum (Figure 3E–F). Conversely, reduced growth was observed at 16 °C and higher temperatures. Light intensity similarly influenced cell growth. Cultures exposed to 60–140 μmol photons m^{-2} s^{-1} showed significantly greater cell densities than low-light treatments, with maximal cell density achieved at 100 μmol photons m^{-2} s^{-1} (Figure 3C, G–H). While SGR remained stable across light treatments (Figure 3D), fluorescence intensity increased under optimal irradiance.

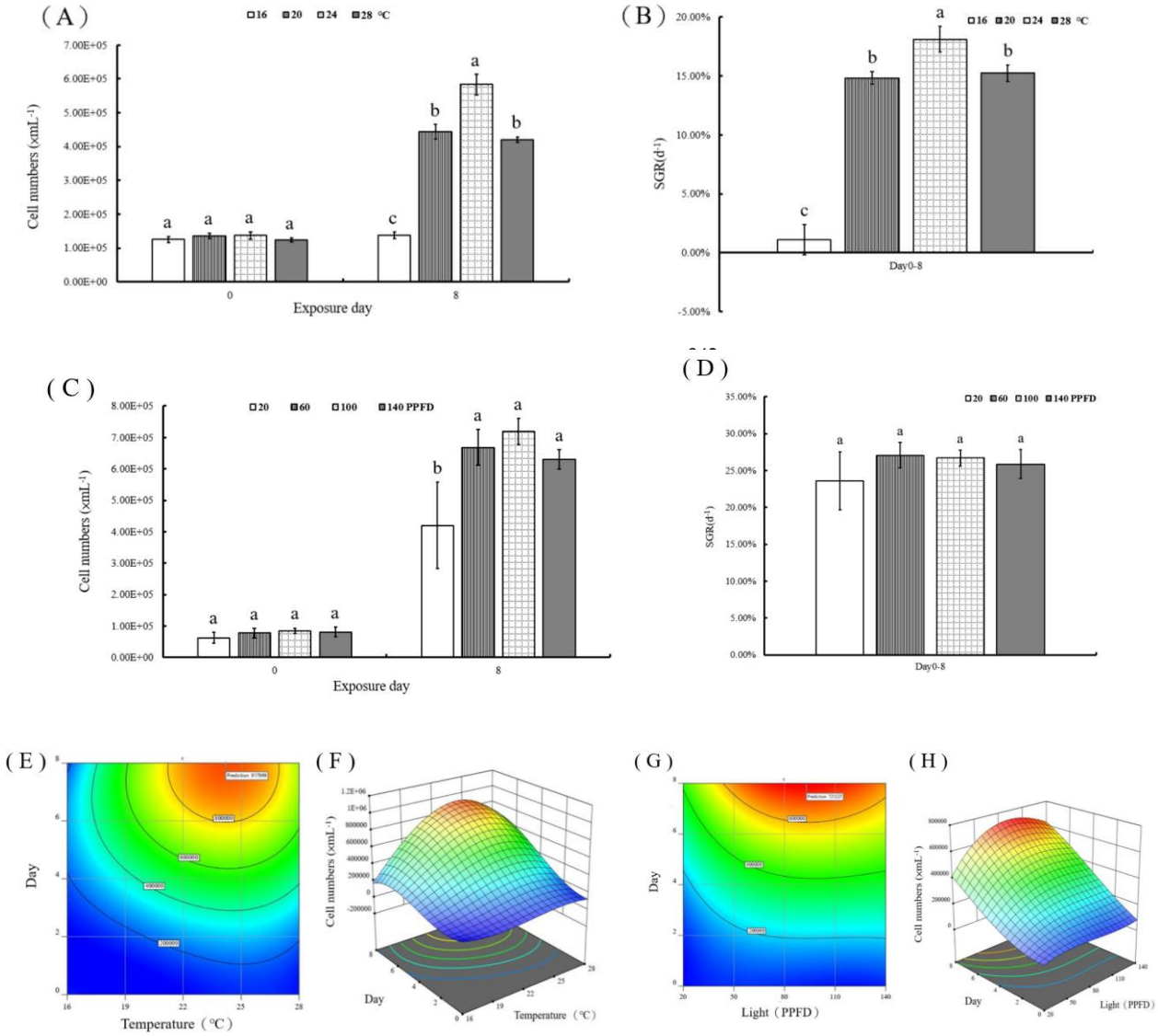
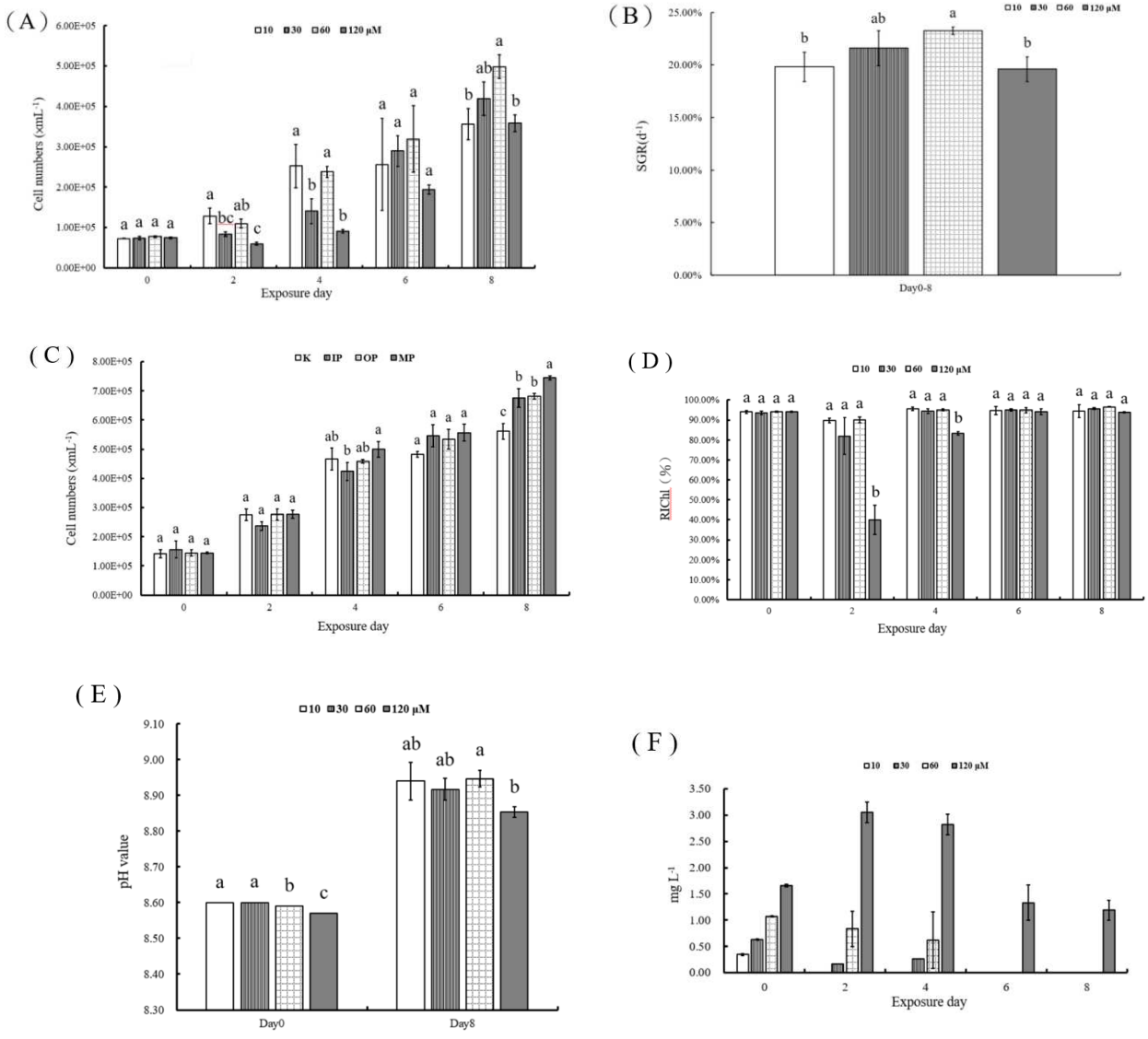


Figure 3. Effects of temperature and light intensity on the growth responses of *Heterocapsa pygmaea*. (A–B) Cell density and specific growth rate (SGR) under different temperature conditions. (C–D) Cell density and SGR under varying light intensities. (E–F) Response surface contours and three-dimensional plots showing the effect of temperature on biomass

production. (G–H) Response surface contour and three-dimensional plots showing the effect of light intensity on biomass production. Different letters indicate significant differences ($p < 0.05$).

3.4. Effects of Phosphorus Concentration and Source on Biomass and PCP-Associated Performance

Phosphorus availability strongly influenced culture productivity and fluorescence responses in *H. pygmaea.* Cultures supplied with 60 μM phosphorus showed the highest cell density and SGR (Figure 4A–B). Cell density over the cultivation period demonstrated better growth at intermediate phosphorus concentrations than under deficient (10 μM) or excess (120 μM) phosphorus treatments (Figure 4C). Low-phosphorus treatments rapidly depleted available phosphorus, whereas residual accumulation at 120 μM indicated reduced utilization efficiency under excess supply (Figure 4F). Under excess phosphorus (120 μM), a transient decline in fluorescence intensity was observed (Figure 4D). Among the phosphorus source treatments, mixed phosphorus (MP) treatments produced the highest fluorescence responses (Figure 4G).



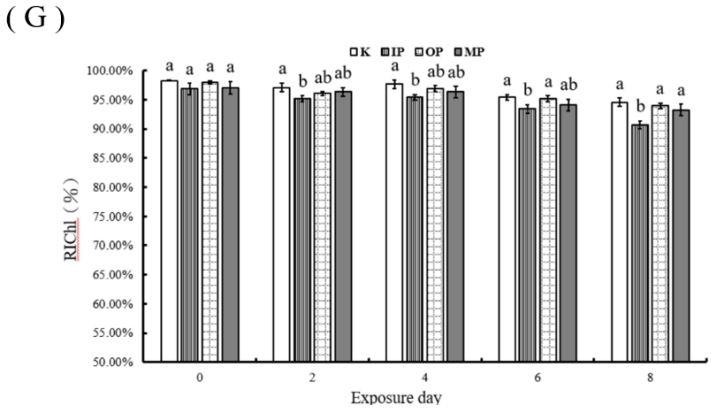
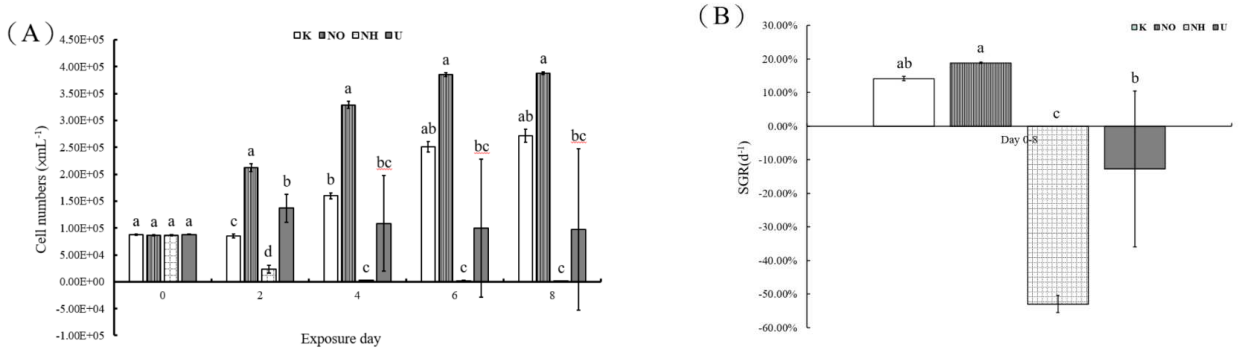


Figure 4. Effects of phosphorus concentration and source on growth, nutrient utilization, and relative fluorescence intensity in *Heterocapsa pygmaea*. (A–B) Cell density and specific growth rate (SGR) under different phosphorus concentrations. (C) Cell density responses to varying phosphorus concentrations throughout the cultivation period. (D) Relative fluorescence intensity (a proxy for PCP-associated performance) under different phosphorus concentrations. (E) pH variation during cultivation. (F) Dynamics of total phosphorus depletion during cultivation. (G) Relative fluorescence intensity under different phosphorus source treatments. Different letters indicate significant differences among treatments ($p < 0.05$).

3.5. Effects of Nitrogen Source and Nitrate–Urea Substitution on Biomass and PCP-Associated Performance

Nitrogen source significantly influenced cell growth and fluorescence responses in *H. pygmaea*. Nitrate and mixed nitrogen treatments produced the highest cell densities and SGR (Figure 5A–B). Ammonium-dominated treatments showed significantly reduced biomass and fluorescence responses (Figure 5A–C). Urea-supported cultures showed similar but less pronounced reductions. The nitrogen source also influenced culture pH, with ammonium-containing treatments showing greater pH variation than nitrate-based treatments (Figure 5D). Notably, partial replacement of nitrate with urea (mixed nitrogen strategy) maintained high cell density and fluorescence performance (Figure 5E–G).



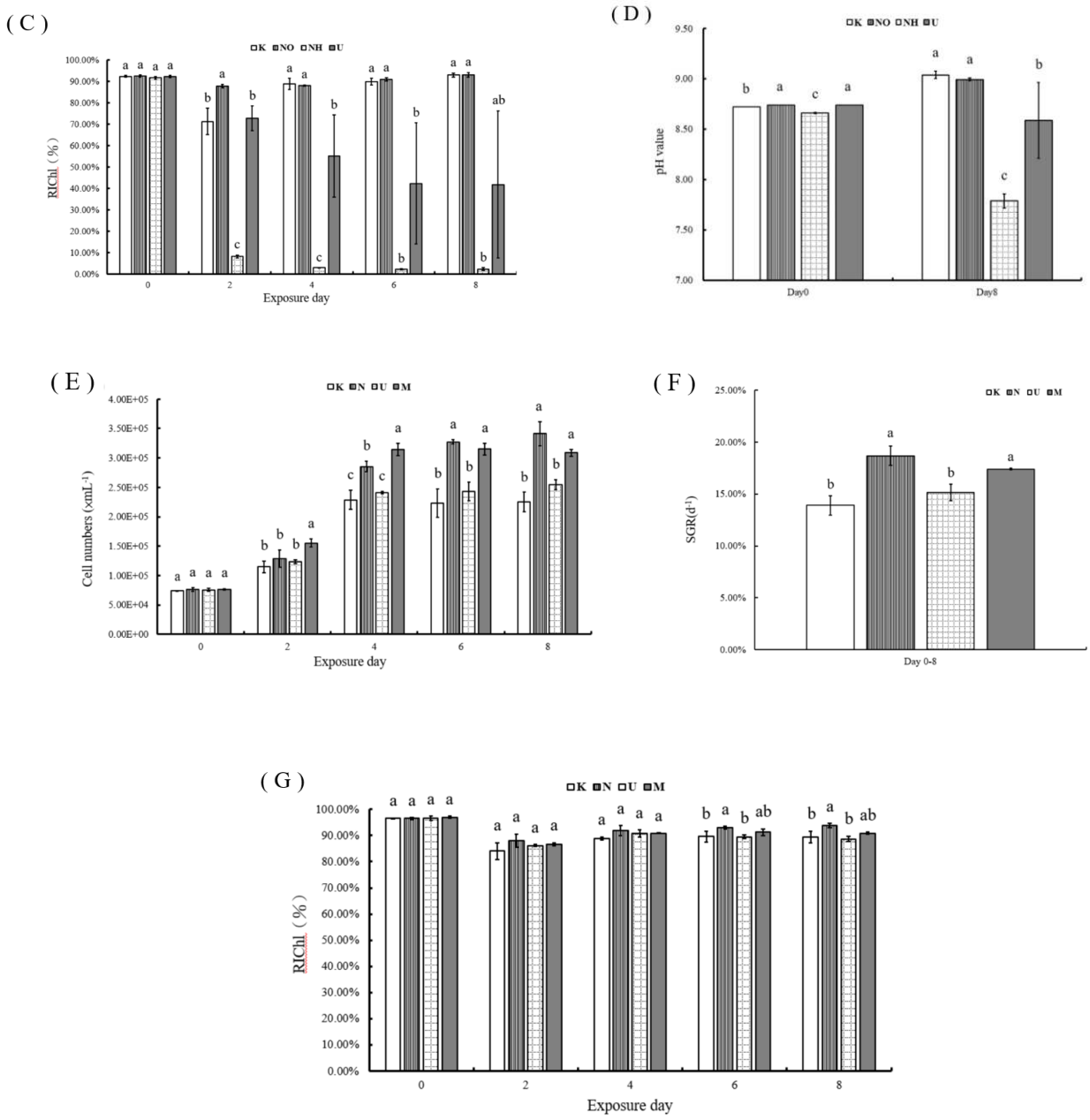


Figure 5. Effects of nitrogen source and nitrate–urea substitution strategy on growth and relative fluorescence intensity of *Heterocapsa pygmaea*. (A–B) Cell density and specific growth rate (SGR) under different nitrogen source treatments. (C) Relative fluorescence intensity under different nitrogen source treatments. (D) pH variation during cultivation. (E–F) Cell density and SGR under different nitrate–urea substitution treatments. (G) Relative fluorescence intensity under different nitrate–urea substitution treatments. Different letters indicate significant differences between treatments ($p < 0.05$).

3.6. Effects of Iron Concentration on Biomass and PCP-Associated Performance

Iron supplementation significantly enhanced cell growth and PCP-associated fluorescence responses in *H. pygmaea*, with the best performance within the tested range observed at 17.55 μM iron, the highest concentration tested (Figure 6A–D, F). Both cell density and specific growth rate increased with iron supplementation up to the highest concentration

tested, and response surface analysis indicated enhanced culture performance under intermediate iron availability (Figure 6A–D). Conversely, iron limitation constrained growth performance. Relative fluorescence intensity was highest under supplementation at 17.55 μM, the highest concentration tested, but temporary fluorescence suppression was observed at elevated iron concentrations followed by a subsequent restoration of fluorescence responses (Figure 6F). Culture pH remained stable across treatments throughout cultivation (Figure 6E).

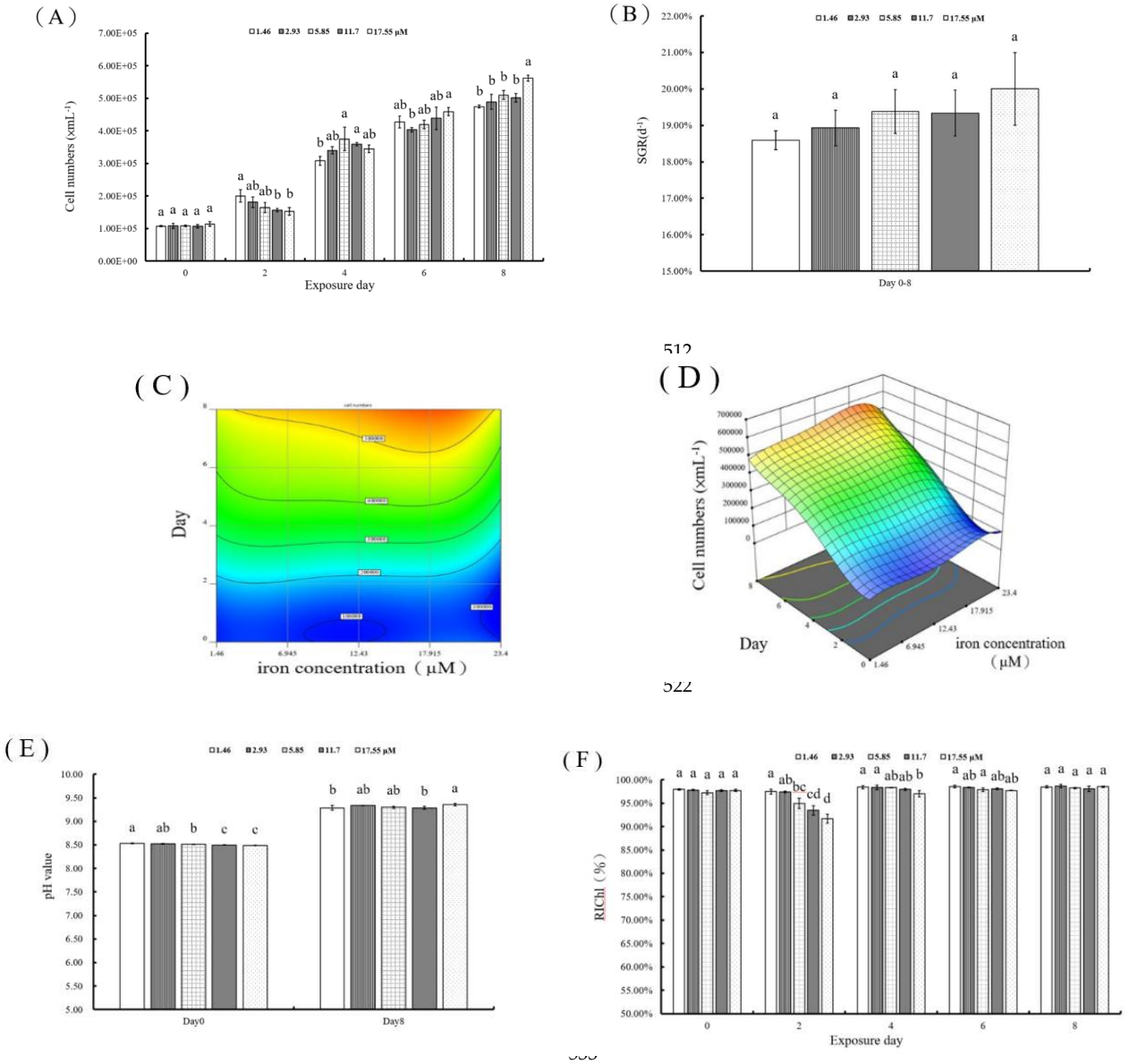


Figure 6. Effects of iron concentration on growth and PCP-associated performance in *Heterocapsa pygmaea*. (A–B) Cell density and specific growth rate (SGR) under different iron concentrations. (C–D) Response surface contour and three-dimensional plots showing the effect of iron concentration on culture productivity. (E) pH variation during cultivation. (F) Relative fluorescence intensity (a proxy for PCP-associated performance) under varying iron concentrations. Different letters indicate significant differences between treatments ($p < 0.05$).

3.7. Validation of Optimized Conditions Using Modified C5 Medium

Integration of optimized environmental and nutritional parameters into the modified C5 medium significantly enhanced cell growth and relative fluorescence intensity compared with conventional f/2 and K media (Figure 7A–C). Relative fluorescence intensity closely paralleled cell growth across the three media (Figure 7C), and representative fluorescence histograms comparing the modified C5 medium with conventional culture media are presented in Supplementary Figure S7. Culture pH remained stable across media formulations throughout cultivation (Figure 7D).

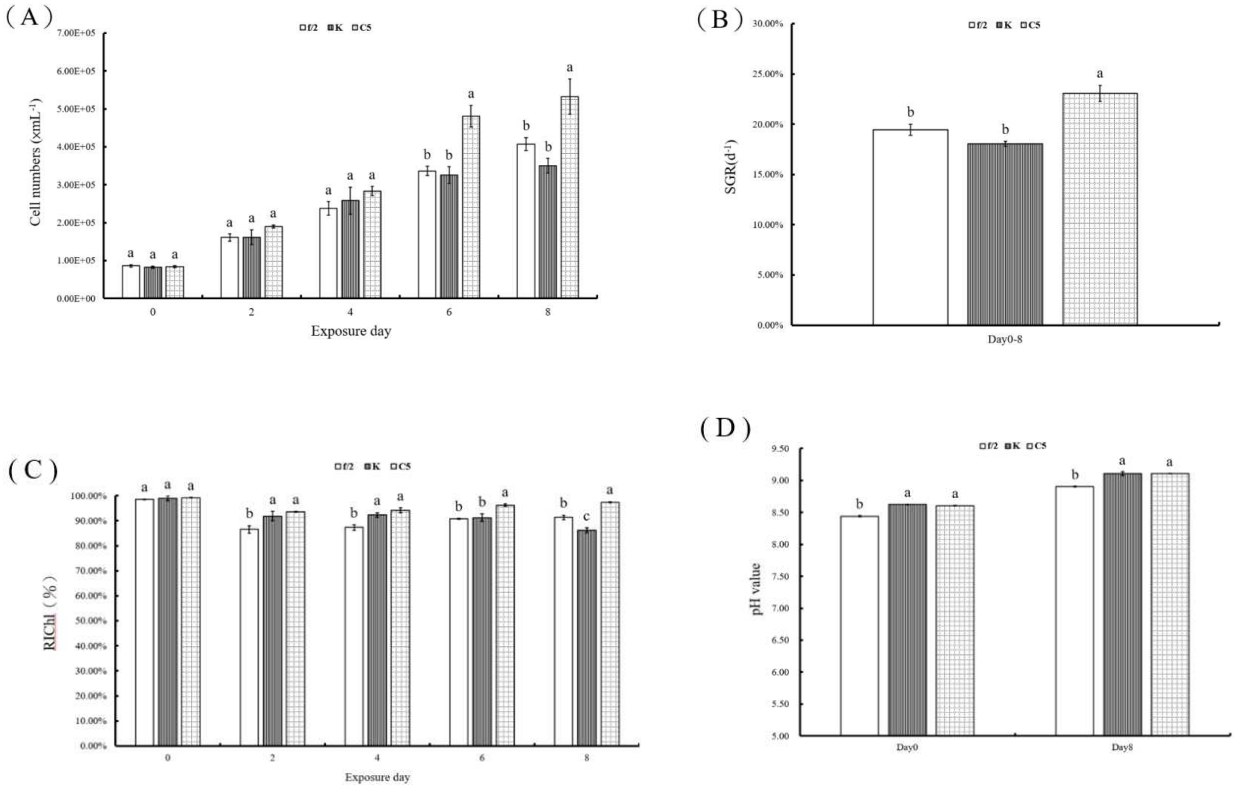


Figure 7. Validation of the optimized cultivation conditions using modified C5 medium. (A–B) Comparison of cell density and specific growth rate (SGR) among C5, f/2, and K media. (C) Relative fluorescence intensity (a proxy for PCP-associated performance) under different culture media. (D) pH variation during cultivation. Different letters indicate significant differences between treatments ($p < 0.05$).

4. Discussion

4.1. Molecular and Pigment Signatures of PCP in Heterocapsa pygmaea

The detection of a 10–15 kDa protein band via SDS-PAGE and the presence of peridinin and chlorophyll a as the major chromophores revealed by RP-HPLC are consistent with previous structural reports of PCP complexes in dinoflagellates [19,22,23]. These individual pigments function as the principal light-harvesting components responsible for expanding the absorption spectrum under blue-green wavelengths, which are predominant in marine environments [20,21]. Together, SDS-PAGE and RP-HPLC support the characterization of the extracted complex as a PCP-type pigment–protein complex, although definitive identification of the protein would require additional evidence, such as the immunological and structural-spectroscopic approaches applied in previous PCP studies [19,22].The structural integrity observed in the extracted complex underscores the feasibility of using *H. pygmaea* as a viable bioresource for industrial or diagnostic fluorescent probes.

4.2. Flow Cytometry as an In Vivo Real-Time Monitoring Tool

Compared with conventional extraction-based quantification methods, which are inherently destructive, labor-intensive, and limit screening throughput, the established FCM framework provides a rapid, single-cell analytical platform for process optimization [10]. The close parallel between cell density and intracellular PerCP fluorescence signals supports the use of cytometric fluorescence as a practical relative indicator of PCP-associated fluorescence responses. Furthermore, the detection of transient fluorescence variations during nutrient stress underscores the sensitivity of FCM in identifying sub-lethal physiological adjustments before bulk changes in cell density become apparent [11,24,25,40]. It should be noted, however, that cytometric fluorescence provides a relative indicator of PCP-associated signal rather than a direct measure of PCP protein content or production [10,11], and absolute PCP quantification would be required to confirm changes in PCP content.

4.3. Environmental Regulation of Cell Growth

The optimization of physical factors revealed that *H. pygmaea* exhibits typical physiological boundaries observed in marine dinoflagellates. The optimal thermal setting of 24 °C supports balanced metabolic activity, whereas lower temperatures (16 °C) restrict enzyme kinetics and higher temperatures induce cellular stress that disrupts growth pathways [14,26,41]. Similarly, the light intensity optimum of 100 μmol photons m^{-2} s^{-1} represents a saturation threshold where energy generation via photochemical pathways is maximized without provoking photoinhibition or reactive oxygen species (ROS) accumulation typically driven by excessive irradiance [27,28].

4.4. Macronutrient Assimilation Dynamics (Phosphorus and Nitrogen)

Phosphorus and nitrogen are essential building blocks for microalgal cell division and pigment-protein synthesis. The high performance observed at 60 μM phosphorus reflects an equilibrium where cellular energy transfer (ATP synthesis) is fully supported without incurring the metabolic stress or economic inefficiency associated with excess accumulation [29,39]. The preference for mixed phosphorus sources suggests that *H. pygmaea* can simultaneously activate inorganic uptake mechanics and organic pathways (such as alkaline phosphatase-mediated hydrolysis) to maximize nutrient-use efficiency [30].

Regarding nitrogen, the superior performance supported by nitrate and nitrate-urea mixtures demonstrates steady assimilation kinetics. Although nitrate assimilation requires sequential enzymatic reduction via nitrate and nitrite reductases, the optimized irradiance provided sufficient reducing power to meet this energetic demand [31]. In contrast, ammonium-dominated cultures suffered from intracellular accumulation and associated oxidative stress, a common toxicity syndrome in microalgae that alters proton balance and destabilizes the medium pH [32,33]. The success of the nitrate-urea substitution highlights a practical strategy for reducing formulation costs in large-scale bioprocesses.

4.5. Micronutrient Impacts and Bioprocess Validation

The strong response to iron supplementation up to 17.55 μM, the highest concentration tested, highlights the role of iron as an indispensable cofactor for electron transport chains (PSI and PSII), ferredoxin, and nitrogen-assimilating enzymes [34,35,37,38]. The transient suppression of fluorescence under excess iron reflects a classic cellular redox adjustment to counter temporary ROS generation, followed by physiological acclimation [36].

The superior performance of the modified C5 medium validates this integrated approach. By avoiding single-factor optimization bias and simultaneously tuning temperature, irradiance, macro-, and micronutrients, the C5 medium achieves metabolic synergy. Enhanced growth was seamlessly coupled with elevated light-harvesting efficiency, presenting a scalable and highly efficient framework for dinoflagellate-based biotechnology.

4.6. Integration and Validation of the Optimized Bioprocess Conditions

These results confirm that coordinated optimization of temperature, light, phosphorus, nitrogen, and iron substantially improves culture performance and PCP-associated cellular responses in *H. pygmaea*. The superior performance of C5 resulted from improved coordination among phosphorus metabolism, nitrogen assimilation, and photosynthetic electron transport: adequate phosphorus supported ATP production and cell division, nitrate-dominant conditions stabilized nitrogen metabolism, and elevated iron enhanced electron transport efficiency [34,35,37,38]. This concordance between cell density and fluorescence responses further supports the usefulness of flow cytometry-guided monitoring for the rapid assessment of culture performance during process optimization. The stability of culture pH across media formulations further suggests that the improved performance of the modified C5 medium was primarily associated with an optimized nutrient composition rather than with substantial differences in culture chemistry. Collectively, this study establishes an integrated dinoflagellate bioprocess optimization framework that combines environmental and nutritional optimization with real-time fluorescence-based physiological assessment. This approach provides a scalable strategy for improving PCP-associated fluorescence responses and highlights the broader application of FCM-guided monitoring in microalgal biotechnology and industrial bioprocess development.

5. Conclusions

This study demonstrates that optimizing environmental and nutritional parameters significantly enhanced cell growth and PCP-associated fluorescence responses in *H. pygmaea*. The best-performing cultivation conditions within the tested ranges were 24 °C, 100 μmol photons m^{-2} s^{-1}, 60 μM phosphorus supplied from mixed sources, nitrate, or mixed nitrogen conditions, and 17.55 μM iron, the highest iron concentration tested. Under these conditions, the modified C5 medium consistently outperformed conventional f/2 and K media in supporting growth and PCP-associated physiological performance.

Biochemical characterization supported the presence of a PCP-type complex, with SDS-PAGE and HPLC analyses revealing the characteristic molecular weight and a pigment composition dominated by peridinin and chlorophyll a. Flow cytometry proved to be an effective in vivo monitoring platform, enabling rapid assessment of cell growth and PCP-associated fluorescence responses under multiple cultivation conditions.

By combining cultivation optimization with fluorescence-based physiological monitoring, this study establishes a practical framework for improving PCP-associated fluorescence performance in *H. pygmaea.* These findings provide a foundation for the scalable cultivation of PCP-producing dinoflagellates and demonstrate the broader value of flow cytometry-guided monitoring as a high-throughput tool for microalgal bioprocess development and industrial biotechnology.

Author Contributions:

Conceptualization, J.-T.L.C., C.-C.H. and M.-C.L.; methodology, J.-T.L.C., C.-C.H., H.-Y.L., V.R. and J.-D.L.; formal analysis and investigation, J.-T.L.C., C.-C.H., Y.-J.C., F.-T.A.S. and Y.-L.C.; writing—original draft preparation, J.-T.L.C., V.R. and C.-C.H.; writing—review and editing, F.-H.N., M.J.L.-A., V.R. and M.-C.L.; funding acquisition, not applicable; resources, M.-C.L.; supervision, M.J.L.-A. and M.-C.L. All authors have read and agreed to the published version of the manuscript.

Funding:

This research received no external funding.

Institutional Review Board Statement:

Not applicable.

Informed Consent Statement:

Not applicable.

Acknowledgments:

The authors sincerely thank the Algal Cultivation and Biotech Laboratory for their invaluable technical assistance and support throughout this study. We also gratefully acknowledge the Norwegian Culture Collection of Algae (NORCCA, Norway) for providing the microalgal strain *Heterocapsa pygmaea* used in this research.

Conflicts of Interest:

The authors declare no conflict of interest.

References

1. Keller, M.D.; Selvin, R.C.; Claus, W.; Guillard, R.R.L. Media for the culture of oceanic ultraphytoplankton. *J. Phycol.* **1987***, 23*, 633–638.

2. Laemmli, U.K. Cleavage of structural proteins during the assembly of the head of bacteriophage T4. *Nature* **1970***, 227*, 680–685.

3. Chen, P.-Y.; Ko, J.-T.; Chen, T.-L.; Ho, M.-Y. Previously unrecognized diversity of far-red light-using terrestrial green algae and cyanobacteria. iSci ence 2025, 28, 113486.

4. Bezerra, M.A.; Santelli, R.E.; Oliveira, E.P.; Villar, L.S.; Escaleira, L.A. Response surface methodology (RSM) as a tool for optimization in analytical chemistry. *Talanta* **2008***, 76*, 965–977.

5. Guillard, R.R.L.; Ryther, J.H. Studies of marine planktonic diatoms. I. Cyclotella nana Hustedt, and Detonula confervacea (Cleve) Gran. *Can. J. Microbiol.* **1962***, 8*, 229–239.

6. Marie, D.; Simon, N.; Vaulot, D. Phytoplankton cell counting by flow cytometry. In *Algal Culturing Techniques*; Andersen, R.A., Ed.; Elsevier: Amsterdam, The Netherlands, **2005**; pp. 253–267.

7. Wood, A.M.; Everroad, R.C.; Wingard, L.M. Measuring growth rates in microalgal cultures. In *Algal Culturing Techniques*; Andersen, R.A., Ed.; Elsevier: Amsterdam, The Netherlands, **2005**; pp. 269–285.

8. Murphy, J.; Riley, J.P. A modified single solution method for the determination of phosphate in natural waters. *Anal. Chim. Acta* **1962***, 27*, 31–36.

9. Valderrama, J.C. The simultaneous analysis of total nitrogen and total phosphorus in natural waters. *Mar. Chem.* **1981***, 10*, 109–122.

10. Certnerova, D., & Galbraith, D. W. Best practices in the flow cytometry of microalgae. *Cytometry* **2021**, Part *A*, *99*(4), 359-364.

11. Hyka, P.; Lickova, S.; Pribyl, P.; Melzoch, K.; Kovar, K. Flow cytometry for the development of biotechnological processes with microalgae. *Biotechnol. Adv.* **2013***, 31*, 2–16.

12. Dębowski, M.; Kazimierowicz, J.; Zieliński, M. Multi-sensing monitoring of the microalgae biomass cultivation systems for biofuels and added value products synthesis—Challenges and opportunities. *Appl. Sci.* **2025***, 15*, 7324.

13. Kana, T.M.; Geider, R.J.; Critchley, C. Regulation of photosynthetic pigments in micro-algae by multiple environmental factors: a dynamic balance hypothesis. *New Phytol.* **1997***, 137*, 629–638.

14. Yamashita, K.; Suzuki, K.; Tokunaga, E. Novel insight into pigment's synthesis and accumulation in microalgae under environmental stress. In *Pigments from Microalgae Handbook—Volume I: Biological Foundations, Environmental Influences and Analytical Methods*; Springer Nature: Cham, Switzerland, **2026**; Volume 1, pp. 185–212.

15. Niedzwiedzki, D.M.; Jiang, J.; Lo, C.; Blankenship, R.E. Low-temperature spectroscopic properties of the Peridinin–chlorophyll a–protein (PCP) complex from the coral symbiotic dinoflagellate *Symbiodinium*. *J. Phys. Chem. B* **2013***, 117*, 11091–11099.

16. Carbonera, D.; Di Valentin, M.; Spezia, R.; Mezzetti, A. The unique photophysical properties of Peridinin–chlorophyll a–protein. *Curr. Protein Pept. Sci.* **2014***, 15*, 332–350.

17. Di Caprio, F.; Posani, S.; Altimari, P.; Concas, A.; Pagnanelli, F. Single cell analysis of microalgae and associated bacteria flora by using flow cytometry. *Biotechnol. Bioprocess Eng.* **2021***, 26*, 898–909.

18. Novoveská, L.; Nielsen, S.L.; Eroldoğan, O.T.; Haznedaroglu, B.Z.; Rinkevich, B.; Fazi, S.; Robbens, J.; Vasquez, M.; Einarsson, H. Overview and challenges of large-scale cultivation of photosynthetic microalgae and cyanobacteria. *Mar. Drugs* **2023***, 21*, 445.

19. Govind, N.S.; Roman, S.J.; Iglesias-Prieto, R.; Trench, R.K.; Triplett, E.L.; Prézelin, B.B. An analysis of the light-harvesting Peridinin–chlorophyll a–protein from dinoflagellates by immunoblotting techniques. *Proc. R. Soc. Lond. B Biol. Sci.* **1990***, 240*, 187–195.

20. Prézelin, B.B.; Haxo, F.T. Purification and characterization of Peridinin–chlorophyll a–proteins from the marine dinoflagellates *Glenodinium* sp. and *Gonyaulax polyedra*. *Planta* **1976***, 128*, 133–141.

21. Hofmann, E.; Wrench, P.M.; Sharples, F.P.; Hiller, R.G.; Welte, W.; Diederichs, K. Structural basis of light harvesting by carotenoids: Peridinin-chlorophyll-protein from *Amphidinium carterae*. *Science* **1996***, 272*, 1788–1791.

22. Schulte, T.; Magdaong, N.C.M.; Di Valentin, M.; Agostini, A.; Tait, C.E.; Niedzwiedzki, D.M.; Carbonera, D.; Hofmann, E. Structural and spectroscopic characterization of the Peridinin–chlorophyll a–protein (PCP) complex from *Heterocapsa pygmaea* (HPPCP). *Biochim. Biophys. Acta Bioenerg.* **2025***, 1866*, 149510.

23. Qiu, S.; Yuan, Y.; Li, X.; Zhao, C.; He, Y.; Tang, B.; Wang, W.; Fan, J. Peridinin–chlorophyll a–protein complex industry from algae: A critical review of the current advancements, hurdles, and biotechnological potential. *Algal Res.* **2023**, *72*, 103118.

24. Jiao, Y.; Ouyang, H.L.; Jiang, Y.J.; Kong, X.Z.; He, W.; Liu, W.X.; Yang, B.; Xu, F.L. Effects of phosphorus stress on the photosynthetic and physiological characteristics of *Chlorella vulgaris* based on chlorophyll fluorescence and flow cytometric analysis. *Ecol. Indic.* **2017**, *78*, 131–141.

25. Liu, Y.; Liu, X.; Nan, F.; Liu, Q.; Lv, J.; Feng, J.; Xie, S. Fe(III)-mediated changes in microalgae-associated bacterial communities and dissolved organic matter characteristics: A case study for *Chlorococcum* sp. GD. *Algal Res.* **2024**, *82*, 103637.

26. Trigueros, M.; Orive, E. Seasonal variations of diatoms and dinoflagellates in a shallow, temperate estuary, with emphasis on neritic assemblages. *Hydrobiologia* **2001**, *444*, 119–133.

27. Shen, A.; Ma, Z.; Jiang, K.; Li, D. Effects of temperature on growth, photophysiology, Rubisco gene expression in *Prorocentrum donghaiense* and *Karenia mikimotoi*. *Ocean Sci. J.* **2016**, *51*, 581–589.

28. Zhang, H.; Gu, B.; Zhou, Y.; Ma, X.; Liu, T.; Xu, H.; Xie, Z.; Liu, K.; Wang, D.; Xia, X. Multi-omics profiling reveals resource allocation and acclimation strategies to temperature changes in a marine dinoflagellate. *Appl. Environ. Microbiol.* **2022**, *88*, e0121322.

29. Huang, X.L.; Zhuang, Y.Q.; Xiong, Y.Y.; Li, D.W.; Ou, L.J. Efficient modulation of cellular phosphorus components in response to phosphorus deficiency in the dinoflagellate *Karenia mikimotoi*. *Appl. Environ. Microbiol.* **2023**, *89*, e0086723.

30. Oh, S.J.; Kwon, H.K.; Noh, I.H.; Yang, H.S. Dissolved organic phosphorus utilization and alkaline phosphatase activity of the dinoflagellate *Gymnodinium impudicum* isolated from the South Sea of Korea. *Ocean Sci. J.* **2010**, *45*, 171–178.

31. Dagenais-Bellefeuille, S.; Morse, D. Putting the N in dinoflagellates. *Front. Microbiol.* **2013**, *4*, 369.

32. Salbitani, G.; Carfagna, S. Ammonium utilization in microalgae: A sustainable method for wastewater treatment. *Sustainability* **2021**, *13*, 956.

33. Wang, Y.; Coyne, K.J. Molecular insights into the synergistic effects of putrescine and ammonium on dinoflagellates. *Int. J. Mol. Sci.* **2024**, *25*, 1306.

34. Hurd, C.L.; Harrison, P.J.; Bischof, K.; Lobban, C.S. Nutrients. In *Seaweed Ecology and Physiology*; Cambridge University Press: Cambridge, UK, 2014; pp. 238–293.

35. Schoffman, H.; Lis, H.; Shaked, Y.; Keren, N. Iron–nutrient interactions within phytoplankton. *Front. Plant Sci.* **2016**, *7*, 1223.

36. Danouche, M.; El Ghatchouli, N.; Arroussi, H. Overview of the management of heavy metals toxicity by microalgae. *J. Appl. Phycol.* **2022**, *34*, 475–488.

37. Doucette, G.J.; Harrison, P.J. Aspects of iron and nitrogen nutrition in the red tide dinoflagellate *Gymnodinium sanguineum*. *Mar. Biol.* **1991**, *110*, 165–173.

38. He, H.; Chen, F.; Li, H.; Xiang, W.Z.; Li, Y.; Jiang, Y. Effect of iron on growth, biochemical composition and paralytic shellfish poisoning toxins production of *Alexandrium tamarense*. *Harmful Algae* **2010**, *9*, 98–104.

39. Li, M.; Shi, X.; Guo, C.; Lin, S. Phosphorus deficiency inhibits cell division but not growth in the dinoflagellate *Amphidinium carterae*. *Front. Microbiol.* **2016**, *7*, 826.

40. Malych, R.; Stopka, P.; Mach, J.; Kotabová, E.; Prášil, O.; Sutak, R. Flow cytometry-based study of model marine microalgal consortia revealed an ecological advantage of siderophore utilization by the dinoflagellate *Amphidinium carterae*. *Comput. Struct. Biotechnol. J.* **2022**, *20*, 287–295.

41. Trigueros, M.; Ansotegui, A.; Orive, E. Remarks on morphology and ecology of recurrent dinoflagellate species in the estuary of Urdaibai (northern Spain). *Bot. Mar.* **2000**, *43*, 93–103.